Volume 326, number 1,2,3, 21–24 FEBS 12649 July 1993

A molecular basis for gating mode transitions in human skeletal muscle Na^+ channels

Paul B. Bennett Jr., Naomasa Makita and Alfred L. George Jr.

Departments of Pharmacology and Medicine, Vanderbilt University Medical School, Nashville, TN 37232-2171, USA

Received 14 April 1993; revised version received 14 May 1993

Recombinant sodium channel α subunits expressed in *Xenopus* oocytes display an anomalously slow rate of inactivation that arises from channels that predominantly exist in a slow gating mode [1,2]. Co-expression of Na^+ channel β_1 subunit with the human skeletal muscle Na^+ channel α subunit increases the Na^+ current and induces normal gating behavior in *Xenopus* laevis oocytes. The effects of the β_1 subunit can be explained by an allosterically induced conformational switch of the α subunit protein that occurs upon binding the β_1 subunit. This binding alters the free energy barriers separating distinct conformational states of the channel. The results illustrate a fundamental modulation of ion channel gating at the molecular level, and specifically demonstrate the importance of the β_1 subunit for gating mode changes of Na^+ channels.

Na^+ channel; I_{Na}; Inactivation; Gating; Subunit

1. INTRODUCTION

Co-expression of brain or muscle recombinant Na^+ channel α subunit with low molecular weight mRNA in *Xenopus* oocytes induces a fast (normal) gating mode and increases the macroscopic Na^+ current without changing the single channel conductance [1,2]. It has been speculated that a modulatory factor encoded in the low molecular weight mRNA may be an enzyme or an accessory peptide such as a β subunit [3]. A recent report indicated that a recombinant β_1 subunit from rat brain increased Na^+ current and induced fast inactivation of rat brain II Na^+ channel α subunits expressed in oocytes [4]. The observed changes in rat brain sodium current upon co-expression with a β_1 subunit may have arisen from an increase in the number of expressed channels or possibly by a change in channel gating, however, the precise mechanism has not been determined. It is not known whether β_1 subunits interact with other Na^+ channel isoforms in general or specifically with the skeletal muscle Na^+ channel. In order to explore the properties and gating mechanisms of human Na^+ channels that may be relevant to human disease states, we have utilized the recently cloned human skeletal muscle Na^+ channel [5] (hSkM1) α subunit and a recombinant β_1 cDNA.

2. MATERIALS AND METHODS

2.1. *PCR cloning of β_1 cDNA*

A rat heart β_1 subunit cDNA was isolated using reverse transcription-PCR cloning. Oligonucleotide PCR primers were designed to amplify a 696 bp cDNA corresponding to nucleotides 220–915 (entire open reading frame) of the rat brain β_1 subunit [4]. First strand cDNA synthesized from total rat heart RNA using MMLV reverse transcriptase and random primers was used as the template for PCR experiments. Amplified cDNAs were subcloned directionally into pBluescript and sequenced. The sequence of one subclone (pRHβ-M6) was identical to the published sequence of rat brain β_1 [4]. Sense β_1-subunit cRNA was transcribed from *Eco*RI linearized pRHβ-M6 using T7 RNA polymerase in the presence of the 5′-cap analog m^7GpppG. Capped α-subunit sense cRNA was transcribed from *Eco*RI linearized pSP64T-hSkM1 using SP6 RNA polymerase.

2.2. *Two-electrode voltage clamp*

Defolliculated oocytes were injected with 40 nl (4–20 ng) of 5′ capped cRNA and were voltage clamped 16–48 h after injection using standard two microelectrode voltage clamp techniques as previously described [6]. The ND-96 bath solution contained (mM): 96 NaCl, 2 KCl, 1.8 $CaCl_2$, 1 $MgCl_2$, 5 HEPES (pH 7.50). Currents were filtered at 5 kHz (−3 dB; 4 pole Bessel filter) and sampled at 50 kHz. Electrodes were filled with 3 M KCl. Electrode resistances were 2–4 MΩ for voltage recording electrodes and 0.15–0.3 MΩ for current passing electrodes. Membrane capacitance was measured by integrating the current induced by small voltage jumps from −100 to −110 mV. Linear leak was subtracted by using a linear least squares regression to leak currents generated between −100 and −60 mV. Membrane capacitance transients were subtracted using a subthreshold scaled signal averaged tracing or a tracing in which channels had been inactivated.

2.3. *Patch clamp recordings*

Outside-out patches were obtained by standard methods [7]. Membrane currents were filtered at 5 kHz (−3 dB) by a four-pole Bessel filter before sampling at 20 kHz. Capacitative and linear leak currents were subtracted by averaging the traces without activity. The patches were superfused with ND-96 solution. The patch electrodes contained (mM): NaF 10, CsF 110, CsCl 20, $MgCl_2$ 2.0, EGTA 2 and HEPES 10; pH 7.35.

2.4. *Data analysis and modelling*

Inactivation curves were fitted with a Boltzmann equation in which

Correspondence address: P.B. Bennett, CC-2209 Medical Center North, Vanderbilt University Medical School, Nashville, TN 37232-2171, USA. Fax: (1) (615) 322 4707.

$V_{1/2}$ represents the half maximal voltage: $y(V) = \{1 + e^{(V-V_{1/2})/s}\}^{-1}$. The time courses of the falling phase of the macroscopic Na^+ current 'apparent inactivation', as well as onset and recovery from inactivation were fitted with exponential functions:
$y(t) = A_\infty + \Sigma\{B_n \cdot \exp(-t/\tau_n)\}$.

Simulations were carried out in FORTRAN on a microcomputer. In this model, a global change in rate constants occurred upon binding of the β_1 subunit such that the forward rate constants were increased and the backward rate constant from the open state was decreased by 5 fold. Each state is separated by an energy barrier the height of which depends exponentially upon thermodynamic factors such as temperature, electrodynamic and electrostatic interactions within the protein as well as the transmembrane electrical field:

$$k_{ij} = \upsilon \cdot \exp(-\Delta G_{ij}/kT)$$

where ΔG_{ij} is the energy barrier height separating states i and j. ΔG contains all factors that contribute to the barrier height including both voltage-dependent and non-voltage-dependent terms. ΔG can be partitioned into a voltage-independent term, ΔG_0, that reflects the barrier height when the field strength is zero, and additional terms that account for the electric field effects. The global change in barrier heights upon binding of the β_1 subunit accounts for both the change in kinetics and the increase in current amplitude. The value of υ is approximately 6×10^{12} s^{-1} and it represents the attempt rate for crossing barriers; it is an upper limit for transition frequencies. At room temperature, RT is 0.582 kcal/mol, thus the activation energy barrier height (well to peak) for a rate constant of 1,000 s^{-1} is 13 kcal/mol. Data are presented as means and standard errors.

3. RESULTS AND DISCUSSION

The first important observation is illustrated in Fig. 1 which demonstrates that the α subunit alone spends a fraction of time in the normal fast gating mode. This was apparent from both the onset of inactivation (Fig. 1A) and its recovery (Fig. 1B). Fig. 1B shows that channels produced by the α subunit alone recover from inactivation very slowly ($38 \pm 1\%$; $\tau_{slow} = 1.2 \pm 0.32$ s, $n = 4$) although a fraction of the channels recover rapidly. However when the α subunit is co-expressed with the β_1 subunit, not only did the current inactivate faster (Fig. 1C), the channels also recover from inactivation rapidly ($88\% \pm 1$; $\tau = 6.5 \pm 0.9$ ms, $n = 4$). Injection of oocytes with β_1 alone had no effect which demonstrates that β_1 alone did not induce expression of an endogenous channel. Fig. 1D shows that β_1 increases the level of Na^+ current compared to the α subunit alone, but only small effects on the apparent voltage dependence of steady state inactivation were observed (α $V_{1/2}$: -51 ± 0.7 mV, $n = 13$; $\alpha + \beta_1$ $V_{1/2}$: -55 ± 0.65 mV, $n = 14$) [4].

To further assess the effects of the β_1 subunit on the magnitude of the expressed Na^+ current, oocytes ex-

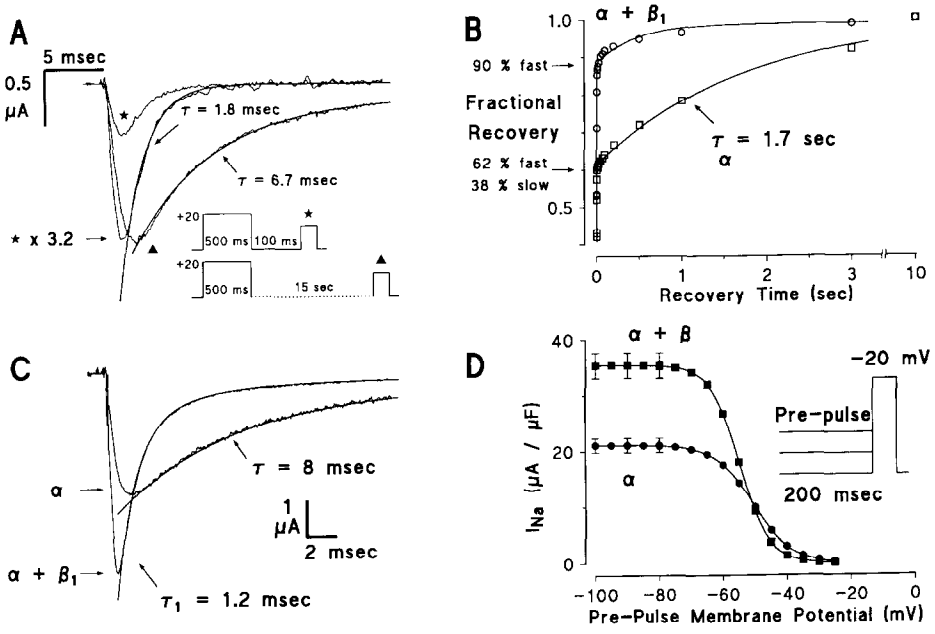

Fig. 1. (A) Superposition of raw current tracings comparing the fast and slow components of inactivation in an oocyte expressing the α subunit alone. Channels were inactivated by a 500 ms pre-pulse and Na^+ current was monitored at 100 ms or 15 s after the pre-pulse. The two modes of kinetic behavior are evident. A brief recovery period revealed a small rapidly inactivating component (star). This component was scaled by a factor of 3.2 in order to compare its inactivation decay with the major slow component seen after a 15 s recovery. The small fast component decayed ~ 4-fold faster than the current in the dominant gating mode ($\tau = 1.8$ vs. $\tau = 6.7$ ms). The scaled tracing was digitally filtered at 3 kHz after scaling. (B) Time course of recovery from inactivation for α subunit alone or for the α subunit coexpressed with β_1. Recovery by the α subunit alone required several seconds although there was always a fast component of recovery. Co-expression with β_1 greatly enhanced the fraction of channels that recovered rapidly. (C) Superposition of raw current tracings comparing the fast and slow components of inactivation (at −20 mV) in an oocyte expressing both the α and β_1 subunit or the α subunit alone. The decaying phase of current was fitted with a bi-exponential equation ($\alpha + \beta_1$) or with a monoexponential (α subunit alone). The inactivating current decayed with a time constant of 8 ms (α alone). Co-expression with the β_1 subunit shifted the gating kinetics such that the major (90%) fraction of channels inactivated rapidly ($\tau = 1.2$ ms). (D) Voltage dependence of channel availability for opening. A standard twin pulse protocol was used to inactivate channels and determine the fractional current following a pre-pulse to different membrane potentials (abscissa).

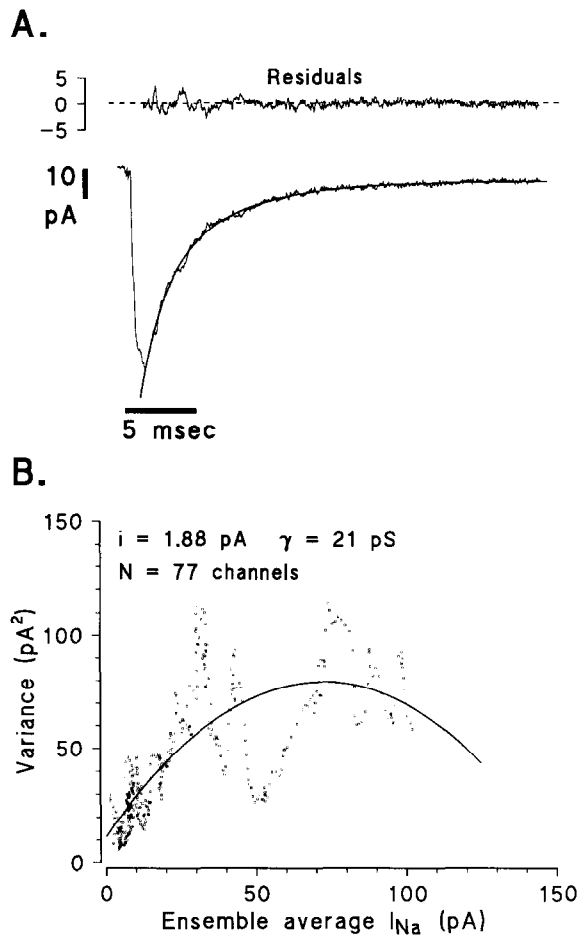

Fig. 2. Outside-out patches excised from an oocyte injected with hSkM1 $\alpha + \beta_1$ subunit cRNA. (A) Ensemble averaged current records demonstrating rapid macroscopic inactivation. The fast component was dominant and decayed with a time constant of 1.5 ms. (B) Non-stationary fluctuation analysis of hSKM-1 $\alpha + \beta_1$ induced Na^+ current. Ensemble variance < VAR > is plotted as a function of the averaged current, < I >. Data were fitted with the following equation $< VAR > = I_i - I^2/N$ (solid curve through data) [15].

pressing α alone or $\alpha + \beta_1$ were voltage clamped alternatively within a 6 h period. The normalized current density (at −20 mV) was significantly ($P < 0.01$) increased during co-expression of the α and β_1 subunits: α subunit 21.1 ± 1.3 μA/μF, $n = 14$; $\alpha + \beta_1$ 35.4 ± 2.3 μA/μF, $n = 13$. In additional experiments using different batches (2) of oocytes and different membrane potentials, the normalized membrane conductance was increased from 0.58 ± 0.12 mS/μF to 1.3 ± 0.26 mS/μF ($n = 12$, $P < 0.05$). We could not account for these increases in macroscopic Na^+ current by an increase in the single channel conductance. Excised patch clamp experiments were performed on oocytes expressing the $\alpha + \beta_1$ subunits in order to determine the single-channel conductance. Fig. 2A shows an ensemble averaged current recorded from an outside-out membrane patch. These channels exhibited fast gating behavior and the single channel conductance was 21 pS (Fig. 2B) which is identical to the single-channel conductance of the α subunit alone [2,8].

Our results demonstrate that human skeletal muscle sodium channels do not have an absolute requirement for the β_1 subunit in order to exhibit normal gating behavior (Fig. 1A). Our data show that co-expression of the β_1 and the α subunit produce the same effects as the unknown factor in the low molecular weight mRNA [2]. When the β_1 subunit is co-expressed with the α subunit, the equilibrium between gating modes appears shifted such that the faster gating mode dominates. These two types of macroscopic inactivation arise from gating mode shifts and not from multiple populations of ion channels being expressed since they are seen in patches with a single channel [2].

We considered whether the observed changes in gating kinetics could also account for the increase in peak Na^+ current. Many voltage-gated ion channels from excitable membranes display heterogeneous patterns of behavior referred to as gating modes [9,10]. Gating mode changes play an important role to modify cellular electrical activity in both normal and diseased states of excitable cells [10–13,17,18]. Brain, cardiac and skeletal muscle sodium channels display at least two distinct gating modes [1,10,12,13,16,18] but the fast gating mode is dominant in situ. Simulations using Eyring theory energy barrier models for the gating transition rate constants indicated that the effects of β_1 on both kinetics and current amplitude could be explained entirely by a change in the probability of channel opening upon binding of the β_1 subunit. In the Eyring reaction rate theory, the gating transition rate constants describe the energy barrier heights for a transition from one kinetic state to another. Lowering these barrier heights results in a faster transition. Since gating of the channel involves a rearrangement of atoms in the protein, the structure(s) responsible must achieve sufficient energy from thermal motion or other sources to traverse the energy barrier that separates different states. We estimated the height of these barriers from reaction rate theory by:

$$\Delta G = -RT \cdot \ln(k_{ij}/\upsilon)$$

where $\upsilon = \kappa \cdot kT/h$, k_{ij} is a rate constant, R is the gas constant, k is Boltzmann's constant, T is temperature, κ is a transmission coefficient (assumed to be 1) and h is Planck's constant. We assume that binding of the β_1 subunit induces a global effect on the structure of the α subunit. This is supported by experiments where neurotoxin binding and action at three distinct sites on the channel are modified by β_1 association [3]. During channel activation, if we lower the barrier heights for all forward transition rates by 1.6 kT and increase the transition barrier height for the rate constant leaving the open state by 1.6 kT (~ 0.93 kcal/mol) when the β_1 subunit binds, we can account for changes in gating and current magnitude (Fig. 3). These profound changes in

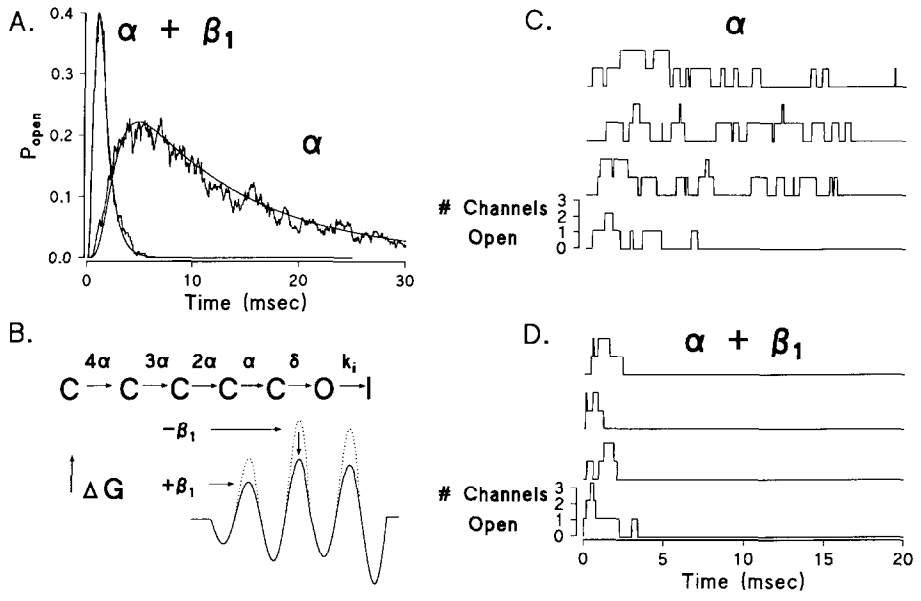

Fig. 3. Simulation of channel gating and the effects of the β_1 subunit based on Eyring rate theory. Channel gating occurs according to a Markov chain model with at least 7 major kinetic states. (A) Ensemble behavior of channel open probability before and after binding of the β_1 subunit. (B) State diagram of an Eryring energy barrier profile for channel gating. Binding of the β_1 subunit lowers the energy barriers for all forward transitions. The backward transition rates were decreased by the same amount (not shown). Upon recovery from inactivation, the rate limiting barrier height was decreased by 2.68 kcal/mol to quantitatively match the data. (C) Single channel behavior in the absence of the β_1 subunit for a patch with three active channels. (D) Single channel behavior in the presence of the β_1 subunit for a patch with three active channels.

channel behavior upon binding the β_1 subunit suggest that relatively small energetic changes are required to extensively modulate gating. The energetic requirement for the changes are less than many reactions that occur readily at room temperature: e.g. carbon–carbon bond rotation (3 kcal/mol), hydrogen bonds (5 kcal/mol) or protonation reactions (2–13 kcal/mol). This result also explains the ability of the α subunit alone to exhibit the fast gating mode albeit less frequently than when the β_1 subunit is present.

Changes in Na^+ channel gating may underlay the aberrant sodium channel behavior seen in human disease states [11] and Na^+ channel mutations are known to occur in patients with these disorders [14,19]. Our results suggest that an additional focus on subunit interactions must also be considered while exploring the mechanisms of ion channel based diseases.

Acknowledgements: We would like to thank Craig Short for performing oocyte microinjections. This work was supported by NIH Grant HL40608 (PBB). PBB is an Established Investigator of the American Heart Association. ALG is a Lucille P. Markey Scholar, and this work was partly supported by a grant from the Lucille P. Markey Charitable Trust.

REFERENCES

[1] Krafte, D.S., Goldin, A.L., Auld, V.J., Dunn, R.J., Davidson, N. and Lester, H.A., (1990) J. Gen. Physiol. 96, 689–706.
[2] Zhou, J., Potts, J.F., Trimmer, J.S., Agnew, W.S. and Sigworth, F.J. (1991) Neuron 7, 775–785.
[3] Messner, D.J., Feller, D.J., Scheuer, T. and Catterall, W.A. (1986) J. Biol. Chem. 261, 14882–14890.
[4] Isom, L.L., De Jongh, K.S., Patton, D.E., Reber, B.F.X., Offord, J., Charbonneau, H., Walsh, K., Goldin, A.L. and Catterall, W.A. (1992) Science 256, 839–842.
[5] George, A.L., Komisarof, J., Kallen, R.G. and Barchi, R.L. (1992) Ann. Neurol. 31, 131–137.
[6] Po, S.S., Roberds, S.L., Snyders, D.J., Tamkun, M.M. and Bennett, P.B. (1993) Circ. Res. 72, 1326–1336.
[7] Hamill, O.P., Marty, A., Neher, E., Sakmann, B., Sigworth, F.J. (1981) Pflügers Arch. 391, 85–100.
[8] Chahine, M., Bennett, P.B., Horn, R. and George, A.L. (1993) Biophys. J. 64, A4.
[9] Hess, P., Lansman, J.B. and Tsien, R.W. (1984) Nature 311, 538–544.
[10] Patlak, J.B. and Ortiz, M. (1986) J. Gen. Physiol. 87, 305–326.
[11] Cannon, S.C., Brown Jr., R.H. and Corey, D.P. (1991) Neuron 6, 619–626.
[12] Nilius, B. (1988) Biophys. J. 53, 857–862.
[13] Patlak, J.B. and Ortiz, M. (1989) J. Gen. Physiol. 94, 279–301.
[14] Ptacek, L.J., George, A.L., Griggs et al. (1991) Cell 67, 1021–1027.
[15] Sigworth, F.J. (1980) J. Physiol. 307, 97–129.
[16] Krafte, D.S., Snutch, T.P., Leonard, J.P., Davidson, N. and Lester, H.A. (1988) J. Neurosci. 8, 2859–2868.
[17] Delcour, A.H. and Tsien, R.W. (1993) Science 259, 980–983.
[18] Kiyosue, T. and Arita, M. (1989) Circ. Res. 64, 389–397.
[19] Rojas, C.V., Wang, J., Schwartz, L.S., Hoffman, E.P., Powell, B.R. and Brown, R.H. (1991) Nature 354, 387–389.